Gastroenterology 2019;■:1–15

Regulation of pH by Carbonic Anhydrase 9 Mediates Survival of Pancreatic Cancer Cells With Activated KRAS in Response to Hypoxia

Q6 **Paul C. McDonald**,[1,*] **Shawn C. Chafe**,[1,*] **Wells S. Brown**,[1,*] Saeed Saberi,[2] Mridula Swayampakula,[1] Geetha Venkateswaran,[1] Oksana Nemirovsky,[1] Jordan A. Gillespie,[1] Joanna M. Karasinska,[3] Steven E. Kalloger,[3] Claudiu T. Supuran,[4] David F. Schaeffer,[3,5] Ali Bashashati,[5] Sohrab P. Shah,[5] James T. Topham,[3] Donald T. Yapp,[6] Jinyang Li,[7] Daniel J. Renouf,[8] Ben Z. Stanger,[7] and Shoukat Dedhar[1,9]

[1]Department of Integrative Oncology, BC Cancer Research Centre, Vancouver, British Columbia, Canada; [2]Department of Molecular Oncology, BC Cancer Research Centre, Vancouver, British Columbia, Canada; [3]Pancreas Centre BC, Vancouver General Hospital, Vancouver, British Columbia, Canada; [4]Department of Chemistry, University of Florence, Florence, Italy; [5]Department of Pathology and Laboratory Medicine, University of British Columbia, Vancouver, British Columbia, Canada; [6]Department of Experimental Therapeutics, BC Cancer Research Centre, Vancouver, British Columbia, Canada; [7]Gastroenterology Division, Department of Medicine and Abramson Family Cancer Research Institute, Perelman School of Medicine, University of Pennsylvania, Philadelphia, Pennsylvania; [8]Medical Oncology, BC Cancer Agency, Vancouver, British Columbia, Canada; and [9]Department of Biochemistry and Molecular Biology, University of British Columbia, Vancouver, BC, Canada

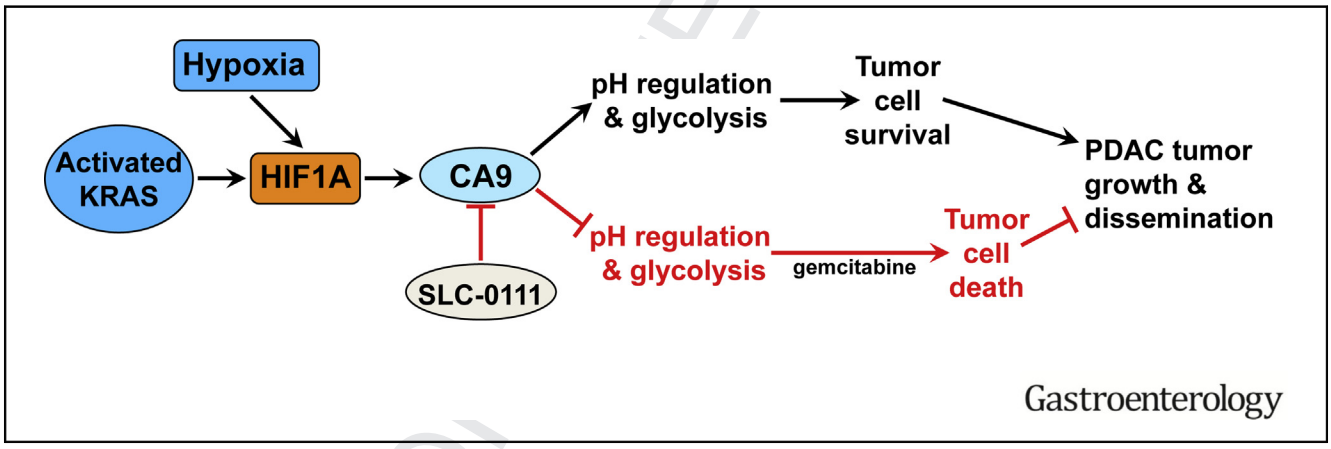

BACKGROUND & AIMS: Most pancreatic ductal adenocarcinomas (PDACs) express an activated form of KRAS, become hypoxic and dysplastic, and are refractory to chemo and radiation therapies. To survive in the hypoxic environment, PDAC cells upregulate enzymes and transporters involved in pH regulation, including the extracellular facing carbonic anhydrase 9 (CA9). We evaluated the effect of blocking CA9, in combination with administration of gemcitabine, in mouse models of pancreatic cancer. **METHODS:** We knocked down expression of KRAS in human (PK-8 and PK-1) PDAC cells with small hairpin RNAs. Human and mouse (*Kras*^{G12D}/*Pdx1-Cre*/*Tp53*/*Rosa*^{YFP}) PDAC cells were incubated with inhibitors of MEK (trametinib) or extracellular signal-regulated kinase (ERK), and some cells were cultured under hypoxic conditions. We measured levels and stability of the hypoxia-inducible factor 1 subunit alpha (HIF1A), endothelial PAS domain 1 protein (EPAS1, also called HIF2A), CA9, solute carrier family 16 member 4 (SLC16A4, also called MCT4), and SLC2A1 (also called GLUT1) by immunoblot analyses. We analyzed intracellular pH (pHi) and extracellular metabolic flux. We knocked down expression of CA9 in PDAC cells, or inhibited CA9 with SLC-0111, incubated them with gemcitabine, and assessed pHi, metabolic flux, and cytotoxicity under normoxic and hypoxic conditions. Cells were also injected into either immune-compromised or immune-competent mice and growth of xenograft tumors was assessed. Tumor fragments derived from patients with PDAC were surgically ligated to the pancreas of mice and the growth of tumors was assessed. We performed tissue microarray analyses of 205 human PDAC samples to measure levels of CA9 and associated expression of genes that regulate hypoxia with outcomes of patients using the Cancer Genome Atlas database. **RESULTS:** Under hypoxic conditions, PDAC cells had increased levels of HIF1A and endothelial PAS domain 1 protein (EPAS1, also called HIF2A), upregulated expression of CA9, and activated glycolysis. Knockdown of KRAS in PDAC cells, or incubation with trametinib, reduced the posttranscriptional stabilization of HIF1A and HIF2A, upregulation of CA9, pHi, and glycolysis in response to hypoxia. CA9

was expressed by 66% of PDAC samples analyzed; high expression of genes associated with metabolic adaptation to hypoxia, including CA9, correlated with significantly reduced survival times of patients. Knockdown or pharmacologic inhibition of CA9 in PDAC cells significantly reduced pHi in cells under hypoxic conditions, decreased gemcitabine-induced glycolysis, and increased their sensitivity to gemcitabine. PDAC cells with knockdown of CA9 formed smaller xenograft tumors in mice, and injection of gemcitabine inhibited tumor growth and significantly increased survival times of mice. In mice with xenograft tumors grown from human PDAC cells, oral administration of SLC-0111 and injection of gemcitabine increased intratumor acidosis and increased cell death. These tumors, and tumors grown from PDAC patient-derived tumor fragments, grew more slowly than xenograft tumors in mice given control agents, resulting in longer survival times. In *Kras*^{G12D}*/Pdx1-Cre/Tp53/Rosa*^{YFP} genetically modified mice, oral administration of SLC-0111 and injection of gemcitabine reduced numbers of B cells in tumors. **CONCLUSIONS:** In response to hypoxia, PDAC cells that express activated KRAS increase expression of CA9, via stabilization of HIF1A and HIF2A, to regulate pH and glycolysis. Disruption of this pathway slows growth of PDAC xenograft tumors in mice and might be developed for treatment of pancreatic cancer.

Keywords: Metabolism; KPCY; Signal Transduction; Transcriptional Regulation.

WHAT YOU NEED TO KNOW

BACKGROUND AND CONTEXT

PDAC is highly hypoxic and chemoresistant, underscoring the urgent need for novel combinatorial therapeutic strategies.

NEW FINDINGS

In response to hypoxia, PDAC cells that express activated KRAS increase expression of carbonic anhydrase 9 (CA9), via stabilization of HIF1A and HIF2A, to regulate pH and glycolysis.

LIMITATIONS

Evaluation of the drug combination on the immune microenvironment remains to be explored in greater detail.

IMPACT

This study identifies CA9 function as a critical vulnerability of KRAS-driven PDAC and demonstrates a novel, clinically tractable, and highly effective combinatorial therapeutic strategy for treatment of patients with pancreatic cancer.

Pancreatic ductal adenocarcinoma (PDAC) is an aggressive malignancy with an extremely poor overall prognosis. Median survival is 6 months, 5-year survival is approximately 9%,[1] and, in the absence of improved outcomes, PDAC is predicted to become the second leading cause of cancer deaths within the next decade.[2] The intractability of this complex disease stems from several factors, including late diagnosis, a paucity of sensitive and specific biomarkers, early dissemination of metastases, and, notably, resistance to chemotherapy, radiotherapy, and currently available targeted therapies.[2]

It is now established that approximately 93% of PDAC tumors harbor mutations in the *KRAS* (Ki-ras2 Kirsten rat sarcoma) oncogene,[3] and many models have demonstrated that mutant KRAS, together with mutations in p53 drive PDAC pathogenesis.[2] However, direct inhibition of KRAS or mutant KRAS has not been tractable to date,[4] and targeting the downstream signaling effectors of RAS, including RAF, mitogen-activated protein kinase kinase (MEK), and extracellular signal-regulated kinase (ERK), has not resulted in significant improvement in the outcome of patients with PDAC.[5]

A major barrier to successful treatment of PDAC is the presence of a complex tumor microenvironment (TME), including hypoxia, a hallmark of many solid tumors that is associated with poor patient prognosis, treatment resistance, and increased invasion and metastasis.[6] Hypoxia is recognized clinically in PDAC,[2] and interrogation of orthotopic patient-derived xenografts (PDX) and genetically engineered mouse models (GEMM) have demonstrated a correlation between increased levels of hypoxia and rapid tumor progression and metastasis.[7,8] Intratumoral hypoxia leads to hypoxia-inducible factor 1 subunit alpha (HIF1A)-mediated metabolic rewiring by cancer cells and the production of acidic metabolites, the accumulation of which impinges on cellular function and viability.[9] To counteract the consequences of an increasingly hypoxic and acidic TME, cancer cells upregulate a network of enzymes and transporters involved in pH regulation, including the extracellular facing carbonic anhydrases (CA) 9 (CA9) and CA12.[10] CA9 is often considered a surrogate marker of tumor hypoxia and is widely regarded as a prominent biomarker of poor patient prognosis for many solid cancers.[11] Several studies have now demonstrated a critical role of CA9 and tumor growth and metastasis.[12,13] CA9 is not widely expressed in normal human tissues, including pancreas, making it an attractive therapeutic target.[14]

Here, we set out to determine whether the oncogenic activation of RAS impinges on the hypoxia response in PDAC. Indeed, we demonstrate that KRAS signaling via MEK and ERK regulates HIF1A and HIF2A protein stability and

* Authors share co-first authorship.

Abbreviations used in this paper: **CA, carbonic anhydrase; DMSO, dimethyl sulfoxide; DOX, doxycycline; ERK, extracellular signal-regulated kinase; GEMM, genetically engineered mouse model; HIF, hypoxia-inducible factor; IP, intraperitoneal; KPCY, *Kras*^{G12D}*/Pdx1-Cre/p53/Rosa*^{YFP}; KRAS, Ki-ras2 Kirsten rat sarcoma; LAMP2, lysosome-associated membrane protein 2; MCT4, monocarboxylate transporter; MEK, Mitogen-activated protein kinase; PDAC, pancreatic ductal adenocarcinoma; PDX, patient-derived xenograft; pHi, intracellular pH; TME, tumor microenvironment; shNS, small hairpin nonsilencing; shRNA, small hairpin RNA.**

0016-5085
https://doi.org/10.1053/j.gastro.2019.05.004

downstream metabolic rewiring results in a switch to a glycolytic phenotype. Among the HIF1A effectors, we have identified CA9 as a key modulator of RAS-driven PDAC progression. We have focused on a multifaceted approach that couples patient data with genetic and pharmacologic strategies in several in vivo models of PDAC, including an orthopically implantable *Kras*-driven GEMM, multiple human xenograft models as well as an orthotopic human PDX model, to evaluate the efficacy of targeting CA9, in combination with gemcitabine, as a tractable therapeutic strategy for Kras-driven PDAC.

Materials and Methods

Ethics Approval and Consent to Participate

Studies using patient materials were carried in accordance with ethics approval obtained from the University of British Columbia Clinical Research Ethics Board (TMA, H12–03484; PDX model, H12–03476).

Animal studies were carried out in accordance with protocols A13–0282 and A17–0291 approved by the Institutional Animal Care Committee at the University of British Columbia, Vancouver and the University of Pennsylvania, Philadelphia.

Exposure to Inhibitors

For MEK inhibitor studies, cells were seeded into 6-well plates (1.5×10^5 cells/well) and allowed to recover overnight. Cells were then cultured without (−) or with (+) 100 nM trametinib (S2673; SelleckChem, Houston, TX) or 1 μM AZD6244 (S1008; SelleckChem) for 72 hours. Cells were cultured either entirely in normoxia (ie, 0 hours of hypoxia) or in normoxia followed by incubation in hypoxia for the times indicated.

For transcription and protein synthesis studies, 10 μM cyclohexamide (14126; Cayman Chemical Co, Ann Arbor, MI) or 10 μM actinomycin D (A1410; Sigma-Aldrich, Oakville, ON, Canada) was added during the final 6 hours of MEK inhibitor exposure.

For proteosome inhibitor studies, 20 μM MG132 (S2619; SelleckChem) was added to cells incubated with trametinib for the indicated times just before cell harvest. For intracellular pH (pHi) measurements, cells were seeded into 96-well plates (5000 cells/well), cultured as described previously for 72 hours, and analyzed using a pHi assay.

All inhibitors were solubilized in dimethyl sulfoxide (DMSO) and equivalent concentrations of DMSO were added to control samples.

Incubation With Gemcitabine and SLC-0111

For in vitro studies, gemcitabine (8941A; Hospira Healthcare, Kirkland, QC, Canada) was diluted in phosphate-buffered saline and added to cell culture media at the indicated final concentrations. SLC-0111 (Welichem Biotech Inc, Burnaby, BC, Canada) was solubilized at 100 mM in DMSO and used at a final concentration of 50 μM. Alternatively, SLC-0111 was solubilized directly in cell culture media at a concentration of 50 μM.

Animal Studies

For studies using PENN 6620c1 clone,[15] 8- to 10-week old female C57Bl/6 mice were anesthetized, the pancreas was surgically exposed, and 30 μL cell suspension (1×10^5 cells/animal) was inoculated. For human cell-line derived xenografts, PK-8 or PK-1 cells (5×10^6 cells/animal) were inoculated subcutaneously on the back of 8- to 11-week old female NOD/SCID or NOD/SCID IL2R$\gamma-/-$ (NSG) mice and tumor volumes were calculated as previously described.[13,16] Drug administration was initiated when tumors reached an average volume of approximately 125 mm^3. For survival analyses, a surrogate threshold was used and survival events occurred once tumors reached approximately 800 mm^3.

For PDX studies, tissue fragments were implanted subcutaneously into male C.B-17 SCID mice (Taconic, Germantown, NY) and grown to 600 to 800 mm^3. Tumors were excised, viable tissue was cut into 6 to 8 fragments and surgically ligated on the pancreas of additional male C.B mice. Tumors from 6 mice were used to generate 40 orthotopic tumors. Tumor growth was determined by palpation 1 time per week using a size scale of 1 to 5. Drug administration was initiated when an average palpation size of 1. Gemcitabine was administered by intraperitoneal (IP) injection using a clinically relevant, 28-day cycle (180 mg/kg 1 time per week for 3 weeks followed by 1-week drug holiday) for 5 cycles. SLC-0111 (50 mg/kg) and vehicle were administered daily by oral gavage until endpoint. Survival was monitored and animals were euthanized when tumors reached the maximum allowable size or as necessitated by comorbidity factors.

For studies involving the $Kras^{G12D}/Pdx1\text{-}Cre/p53/Rosa^{YFP}$ (KPCY) GEMM model of PDAC, male and female mice with tumors approaching 100 mm^3 as assessed by ultrasound were enrolled into the study and randomized into the various groups. Gemcitabine was administered at 120 mg/kg by IP injection 1 time weekly. SLC-0111 (50 mg/kg) and vehicle were administered daily by oral gavage. All animals were administered drugs for 14 days and animals given the combination were administered both drugs concurrently.

Gemcitabine (8941A; Hospira Healthcare) was diluted in sterile saline and administered to animals by IP injection at the indicated doses and duration. SLC-0111 (Welichem Biotech Inc, Burnaby, Canada) was formulated in a clinically validated orally bioavailable emulsion (soy lecithin, vitamin E TPGS, PEG 200, PEG 400, and propylene glycol) and was administered daily by gavage at the indicated doses.

For in vivo studies, mice were not randomized but were instead allocated to different groups based on average tumor volume. The investigators were not blinded to the identity of the groups. The number of animals per group was chosen based on data from previous studies.[13,16]

Full methods are described in the Supplementary Materials and Methods.

Results

KRAS, MEK, and ERK Signaling Promotes Hypoxia-driven HIF1A Protein Stabilization and Expression of CA9, Together With a Metabolic Switch to Glycolysis

Because PDAC is a *KRAS*-driven malignancy and hypoxia is an important component of the TME in PDAC, we interrogated the potential intersection between these critical elements. Analysis of the hypoxia response by *KRAS*-mutant

PK-8 human PDAC cells showed rapid stabilization of HIF1A and HIF2A, followed by upregulation of the HIF1A-induced effector, CA9 (Supplementary Figure 1*A*), compared with a lower level of these proteins in normoxia (0 hours of hypoxia). We engineered PK-8 cells to express doxycycline (DOX)-inducible small hairpin RNAs (shRNAs) targeting *KRAS* or a nonsilencing control (shNS) and examined the effect of KRAS knockdown on the hypoxic response. Incubation of these cells with DOX for 72 hours to induce shRNA expression resulted in robust depletion of RAS expression by shRNAs targeting KRAS cells cultured in normoxia and hypoxia (Figure 1*A* and Supplementary Figure 1*B*). RAS knockdown in hypoxia was coupled with reduced HIF1A levels and inhibition of CA9 expression (Figure 1*A* and Supplementary Figure 1*B*), as well as reduced expression of transcription factor YB1, and the monocarboxylate transporter, MCT4 (Figure 1*A*).

To determine whether KRAS, MEK, and ERK signaling was involved in the regulation of HIF1A and CA9 by PDAC cells cultured in hypoxia, we used the MEK inhibitor, trametinib. Incubation of both human PDAC cells and congenic PDAC tumor cell clones derived from the KPCY GEMM[15] with trametinib for 72 hours resulted, as expected, in the inhibition of ERK phosphorylation, as well as decreased expression of ERK-regulated transcription factors ETS1 and YB1 (Figure 1*B* and *C* and Supplementary Figure 1*C*). Similar to silencing KRAS expression, trametinib exposure was associated with reduced HIF1A levels and its nuclear localization, together with decreased expression of CA9 (Figure 1*B* and *C* and Supplementary Figure 1*C*). Incubation with another MEK inhibitor, AZD6244, similarly inhibited hypoxia-induced upregulation of CA9 (Supplementary Figure 1*D*).

Next, we determined whether RAS, MEK, and ERK signaling regulates HIF1A at the level of transcription or translation to mediate upregulation of CA9 expression. DOX-inducible depletion of *KRAS* expression or incubation with trametinib resulted in a significant reduction of steady-state *HIF-1A* messenger RNA levels in PK-8 cells cultured in normoxia and hypoxia (Supplementary Figure 1*E* and *F*). Incubation of PK-8 cells with actinomycin D, an inhibitor of active transcription, did not impact the hypoxia-induced increase in HIF1A protein (Figure 1*D*), suggesting that transcriptional changes do not account for the loss of HIF-1 protein in the presence of MEK inhibition in hypoxia. In contrast, incubation of cells with protein synthesis inhibitor cyclohexamide completely blocked hypoxia-mediated induction of HIF1A (Figure 1*D*), an effect maintained in the presence of trametinib, suggesting that the KRAS, MEK, and ERK pathway regulates HIF1A posttranscriptionally. As expected, RAS depletion or trametinib exposure resulted in marked reduction of hypoxia-induced *CA9* messenger RNA (Supplementary Figure 1*G* and *H*), consistent with HIF1A-mediated transcriptional regulation of CA9.

Because increased HIF1A and HIF2A expression in hypoxia can occur through protein stabilization, we investigated whether KRAS signaling modulated this pathway. Incubation of PK-8 and PK-1 cells with proteosome inhibitor MG132 in normoxia resulted in accumulation of HIF1A and HIF2A as expected, whereas incubation with trametinib and MG132 resulted in reduced HIF1A accumulation (Figure 1*E* and Supplementary Figure 1*C*). The inhibition of YB1 expression on depletion of KRAS (Figure 1*A*) or MEK inhibition (Figure 1*B*) suggests that this pathway may also regulate HIF1A expression through translation.[17]

Because genetic depletion of KRAS and trametinib exposure blocked HIF1A levels and CA9 expression in hypoxia, we investigated the effects of blocking RAS signaling on metabolic parameters mediated by CA9, such as pHi homeostasis and glycolysis. Both DOX-induced *KRAS* depletion and trametinib exposure resulted in a significant reduction in pHi in PK-8 cells, in normoxia and in hypoxia, compared with control cells (Figure 1*F* and *G*). The decrease in pHi observed with depletion of KRAS was rescued by overexpression of CA9 (Figure 1*H* and Supplementary Figure 1*I*), providing a direct link between the RAS-mediated effect on pHi and CA9 expression. Exposure of PK-8 cells to trametinib also significantly decreased glycolytic function in normoxia and hypoxia (Figure 1*I* and *J*). These metabolic changes were concomitant with inhibition of hypoxia-mediated increases in CA9 (Figure 1*B*), glucose transporter 1, and MCT4 (Figure 1*K*).

Finally, we assessed the effect of *KRAS* depletion on the growth of PDAC spheroids. DOX-induced depletion of *KRAS* in PK-8 cells resulted in significantly smaller spheroids, compared with shNS controls (Figure 1*L*). Thus, one consequence of KRAS inhibition in PDAC cells may be the downregulation of HIF1A-regulated metabolic effectors that compromise glycolytic function and pH regulation in hypoxia and lead to reduced PDAC cell growth.

CA9 Is Upregulated in KRAS-mutant PDAC and Is a Potential Therapeutic Target

Our results described previously, coupled with a previous report demonstrating that the KRAS and HIF1A pathway predicts patient survival in resectable pancreatic cancer,[18] led us to determine whether genes associated with metabolic adaptation by cancer cells to hypoxia were differentially expressed in patients with *KRAS*-driven PDAC and whether expression correlated with clinical outcome. We interrogated data on 135 bona fide *KRAS*-mutant PDAC cases[3] in The Cancer Genome Atlas. Hierarchical clustering of genes previously identified within a hypoxia signature in metastatic breast cancer[13] and known as metabolic regulators of the hypoxic response in PDAC, including *CA9*, identified 2 clusters of patients based on high or low levels of expression of "hypoxia adaptation" genes (Figure 2*A*). A high level of *CA9* expression was significantly associated with the patients in the high hypoxia adaptation cluster (Figure 2*B*) and associations were also identified among other hypoxia response genes used for clustering (Supplementary Figure 2*A*).

Kaplan-Meier analysis of these patient clusters showed that the high hypoxia adaptation cluster was correlated with significantly shorter overall survival (Figure 2*C*). Further examination of the gene expression data identified an additional cluster of patients with very low levels of hypoxia adaptation genes, especially *CA9* (Figure 2*D* and *E* and

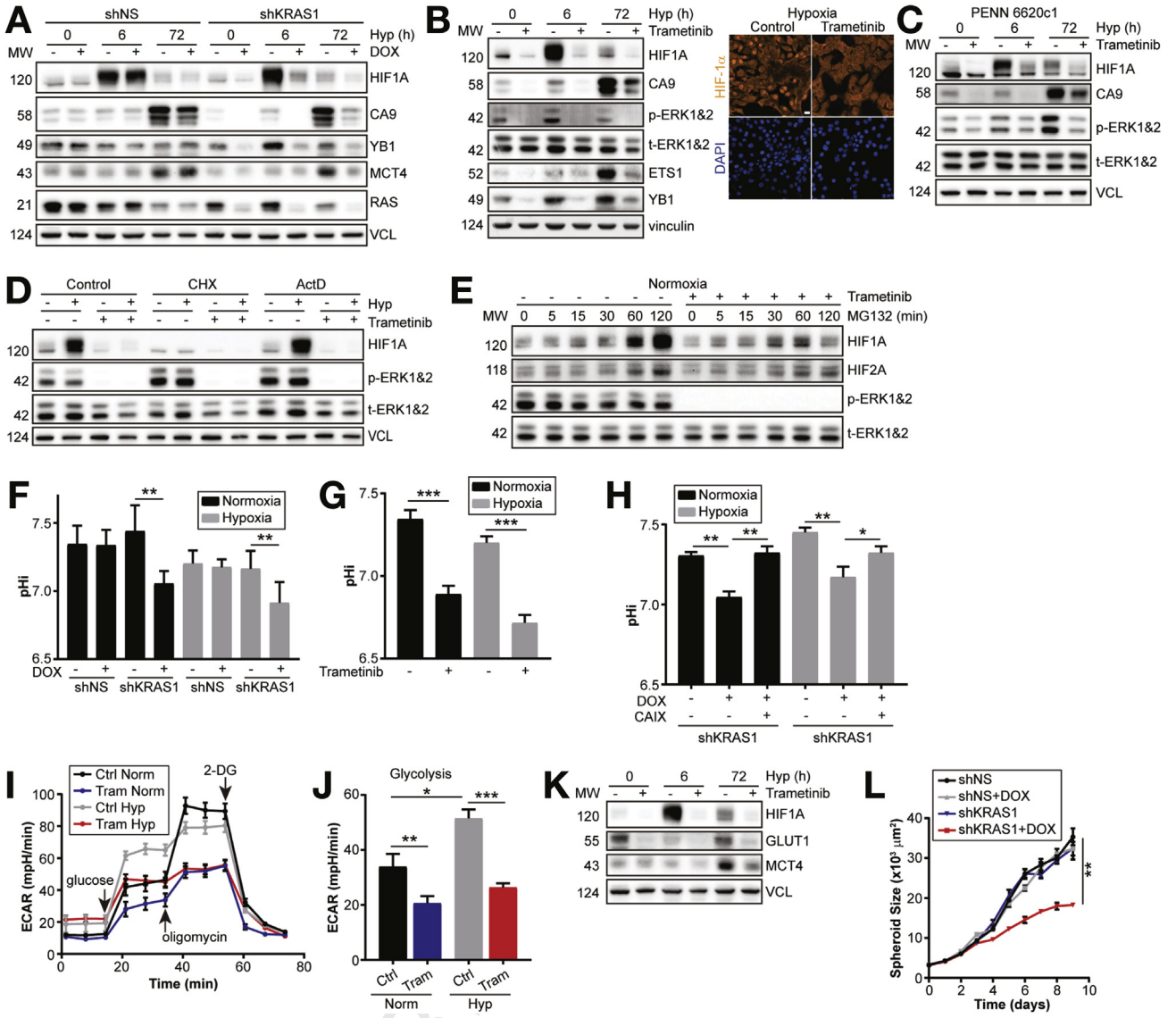

Figure 1. KRAS/MEK AND ERK signaling promotes hypoxia-driven HIF1A stabilization and CA9 expression, together with a metabolic switch to glycolysis. (*A*) Western blots of PK-8 cells grown with (+) or without (−) DOX for 72 hours to induce shRNA and cultured in hypoxia (Hyp) for indicated times. (*B–E*) Western blots of PDAC cells incubated with 100 nM trametinib for 72 hours. (*B*) PK-8 cells cultured in hypoxia as indicated. *Right*: Cells cultured in hypoxia for 6 hours and stained for HIF1A (*orange*) and nuclei (*blue*). Scale bar, 10 μm. (*C*) PENN 6620c1 clone cultured as described in (*B*). (*D*) PK-8 cells cultured for 6 hours in hypoxia with cyclohexamide (10 μM) or actinomycin D (ActD) (10 μM). (*E*) PK-8 cells incubated with MG132 (20 μM). (*F*) pHi measurements for PK-8 cells inducibly depleted of KRAS as described in (*A*) for 72 hours (n = 6, $^{**}P < .01$). (*G*) pHi measurements for PK-8 cells incubated with 100 nM trametinib for 72 hours (n = 6, $^{***}P < .001$). (*H*) pHi measurements for CA9-overexpressing PK-8 cells inducibly depleted of KRAS as described in (*A*) for 72 hours (n = 7, $^{*}P < .05$; $^{**}P < .01$). (*I*) Glycolytic flux of PK-8 cells incubated with as described in (*G*). *Arrows*, compound addition. (*J*) Glycolysis rate calculated from (*I*). (n = 10, $^{*}P < .05$; $^{**}P < .01$; $^{***}P < .001$). (*K*) Western blots of PK-8 cells as described in (*B*). (*L*) Spheroid measurements for PK-8 cells inducibly depleted of KRAS as described in (*A*) and cultured in 3*D*. (n = 3, $^{**}P < .01$).

Supplementary Figure 2*B*), and this group of patients demonstrated significantly longer survival, compared with the clusters with higher levels of gene expression (Figure 2*F*).

We interrogated a tissue microarray containing 205 surgically resectable PDAC cases for CA9 expression. Membranous staining for CA9 was observed on epithelial tumor cells (Figure 2*G*) and CA9-positive tumor cells were detected in 135 (66%) of 205 patients (Supplementary Table 1), showing that CA9 is expressed by a substantial proportion of human PDAC samples.

Finally, to determine whether *CA9* is expressed in metastatic lesions from patients with PDAC, we examined RNA sequencing data generated through a clinical Personalized Oncogenomics Program. Analysis of data from 14 patient samples demonstrated that *CA9* is expressed in metastatic lesions (Figure 2*H*), indicating that CA9 may also be a relevant therapeutic target in PDAC metastases.

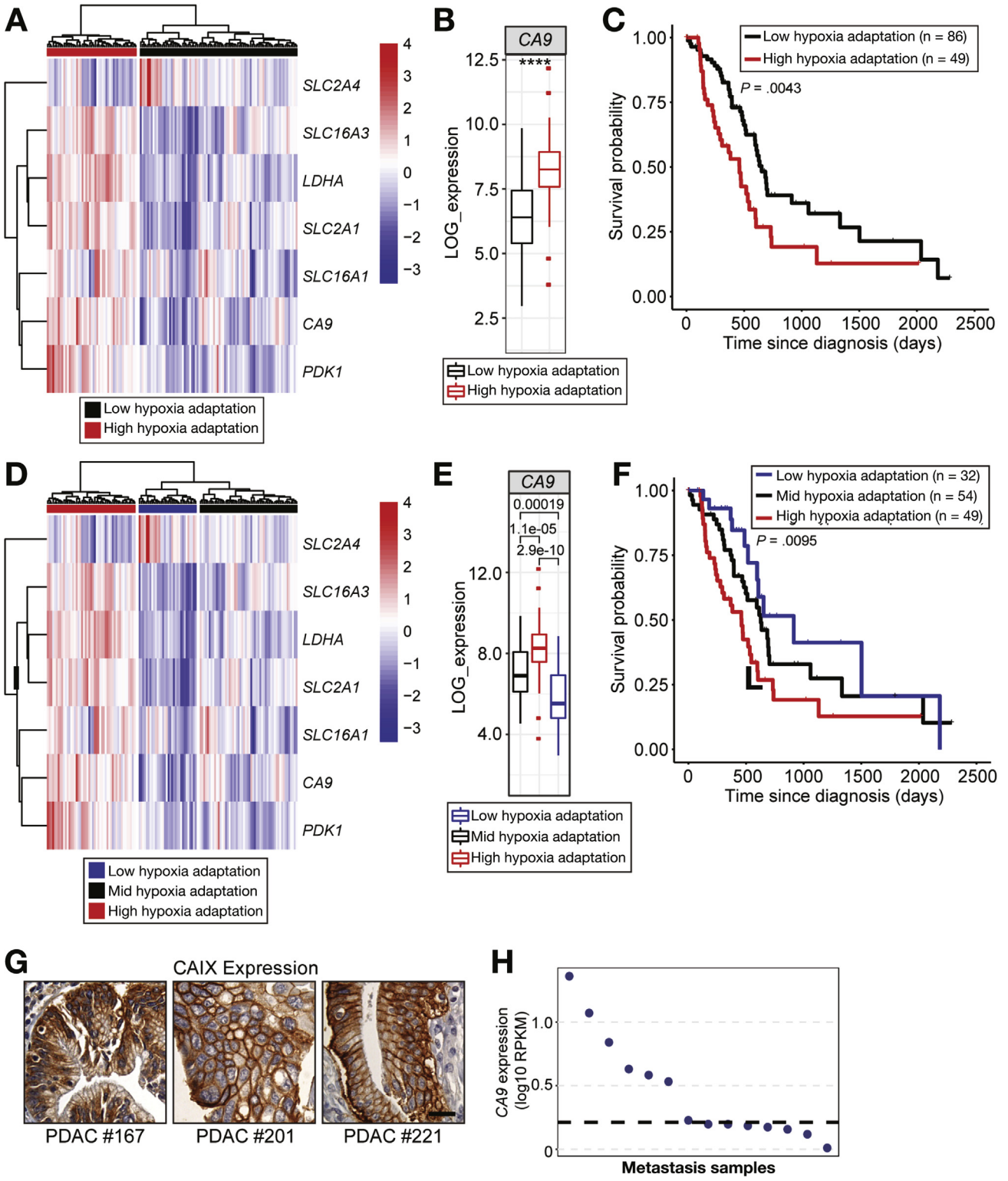

Figure 2. CA9 is upregulated in *KRAS*-mutant PDAC and is a potential therapeutic target. (*A*) Heatmap of curated The Cancer Genome Atlas-PAAD dataset (n = 135) with hierarchical clustering according to high and low gene expression. Scale, *Z*-score. (*B*) Box and whisker plot showing expression values for *CA9* across clusters in (*A*). ****$P < .0001$. (*C*) Kaplan-Meier curves for patients stratified according to clusters defined in (*A*). $P = .0043$. (*D*) Heatmap of the Cancer Genome Atlas-PDAC dataset with hierarchical clustering according to low, mid, and high levels of gene expression. Scale, *Z*-score. (*E*) Box and whisker plot showing expression values for *CA9* across clusters in (*D*). *P* values are indicated. (*F*) Kaplan-Meier curves for patients stratified according to clusters defined in (*D*). $P = .0095$. (*G*) Immunohistochemistry for CA9 expression by PDAC tissue microarray samples. Scale bar, 20 μm. (*H*) RNA sequencing analysis of *CA9* expression in metastatic lesions from patients participating in Personalized Oncogenomics and diagnosed with PDAC. *Dashed line*, median expression.

print & web 4C/FPO

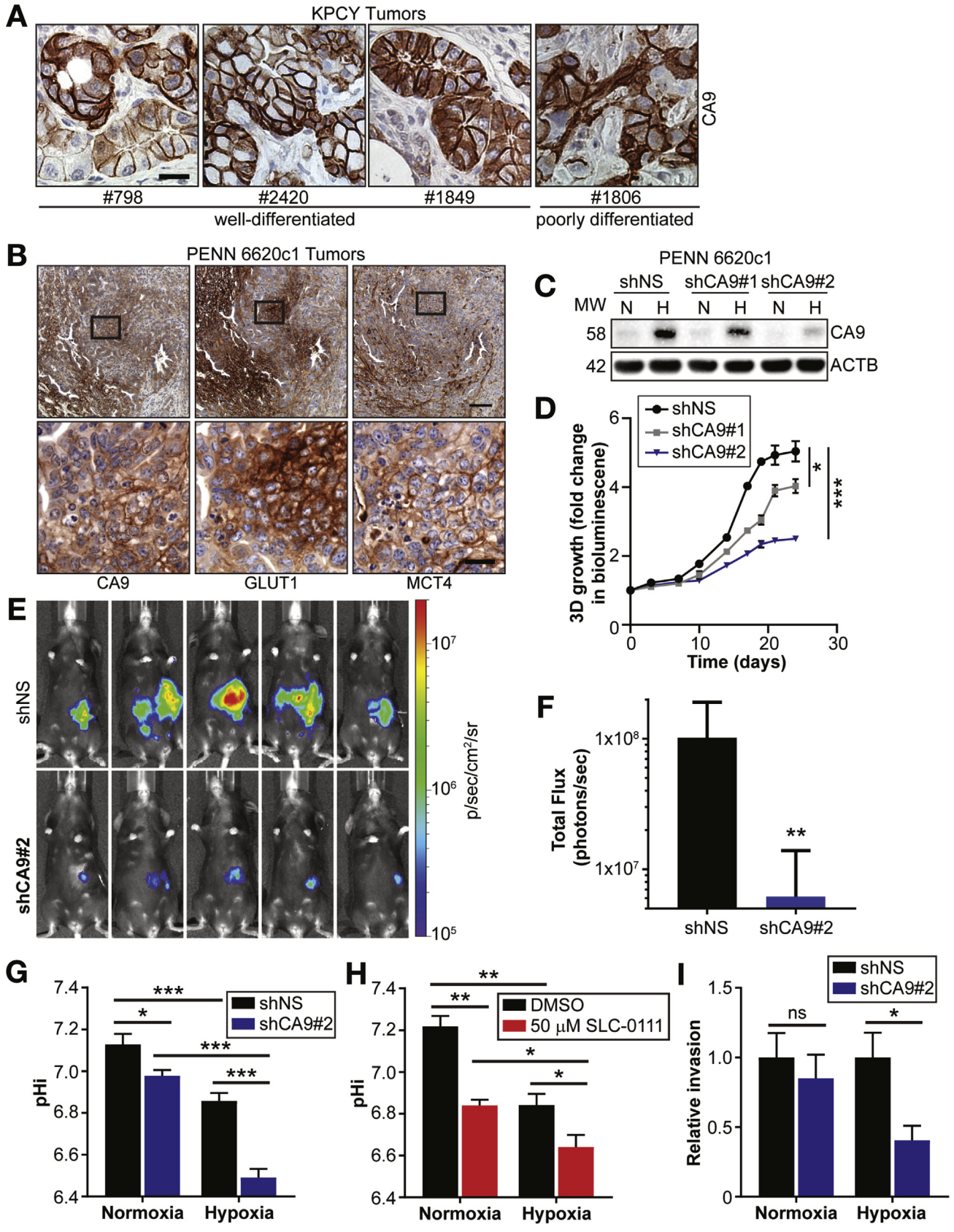

Depletion of CA9 Expression Reduces Tumor Burden and Metastatic Dissemination in a Kras-driven Mouse Model of PDAC

Immunohistochemical analysis of primary tumors arising in the KPCY GEMM of PDAC[15,19] demonstrated membrane-localized expression of CA9 in both well-differentiated and more poorly differentiated tumors (Figure 3*A*). Thus, we focused on studies using cells derived from KPCY mice to evaluate the role of CA9 expression in PDAC tumor growth and dissemination.

Analysis of congenic PDAC tumor cell clones isolated from late-stage KPCY primary tumors[15] in response to hypoxia demonstrated increased levels of HIF1A expression by all clones, whereas several clones, in particular PENN 6620c1, also upregulated CA9 (Supplementary Figure 3*A*). PENN 6620c1 was implanted orthotopically in syngeneic mice and tumors showed heterogeneous, regional staining for CA9, glucose transporter 1 and MCT4, indicating the presence of CA9-positive hypoxic niches (Figure 3*B*). This clone was engineered to express luciferase and was stably depleted of CA9 expression using shRNAs. Western blot analysis demonstrated effective depletion of CA9 compared with control cells (Figure 3*C*), especially using shCA9#2. Knockdown of CA9 expression significantly reduced bioluminescence of these cells when cultured as spheroids in Matrigel (Figure 3*D*), demonstrating that silencing CA9 inhibits growth of these cells.

We introduced shNS and shCA9#2 6620c1 cells orthotopically into syngeneic mice and evaluated the impact of CA9 depletion on PDAC progression in an immune-competent setting. CA9 depletion resulted in a decrease in bioluminescence 21 days postimplantation (Figure 3*E*) and analysis of total flux demonstrated a significant reduction in tumor burden, compared with control tumors (Figure 3*F*). Furthermore, assessment of tissues from these animals ex vivo demonstrated a decrease in grossly visible metastases in animals bearing shCA9#2 tumors, (Supplementary Table 2).

To explore the potential mechanism by which targeting CA9 inhibits tumor growth, the effect of CA9 knockdown on pHi in 6620c1 cells was evaluated. CA9-depleted cells showed a significant reduction in pHi in hypoxia, compared to control cells (Figure 3*G*). Depletion of CA9 also decreased pHi in normoxia (Figure 3*G*), possibly due to basal levels of CA9 expression by these cells (Supplementary Figure 3*A*). Incubation of 6620c1 cells with 50 μM SLC-0111, a clinically validated inhibitor of CA9,[20] in hypoxia also resulted in a significant decrease in pHi (Figure 3*H*). These results show that inhibiting CA9 impairs their ability to regulate pHi in hypoxia, potentially leading to reduced tumor growth and dissemination in vivo.

Finally, we determined the impact of inhibiting CA9 on invasion[21] by PDAC cells. shRNA-mediated depletion of CA9 expression by 6620c1 cells significantly inhibited invasion through Matrigel in hypoxia, but not in normoxia (Figure 3*I*). Incubation of PK-8 cells with 50 μM SLC-0111 also significantly reduced invasion in hypoxia (Supplementary Figure 3*B*), further suggesting the potential therapeutic impact of targeting CA9 in PDAC.

Inhibition of CA9 Interferes With pH Regulation and Inhibits a Gemcitabine-induced Metabolic Stress Response to Enhance Chemosensitivity

Next, we investigated whether inhibiting CA9 would enhance the sensitivity of PDAC cells to gemcitabine, a standard of care chemotherapy for patients with PDAC.[22] We determined the effect of gemcitabine exposure on the viability of PDAC cells using dual-color live-cell imaging. PK-8 cells cultured in hypoxia demonstrated a significantly lower cytotoxicity index with increasing gemcitabine concentration, compared with cells in normoxia (Figure 4*A* and Supplementary Figure 4*A*), demonstrating that hypoxia increases resistance of these cells to gemcitabine. Furthermore, incubation of PK-8 cells with gemcitabine resulted in increased levels of HIF1A and CA9 expression (Figure 4*B* and Supplementary Figure 4*B*).

We carried out studies investigating the impact of silencing *CA9* gene expression in combination with gemcitabine exposure on glycolytic and oxidative metabolism. Analysis of PK-8 cells stably depleted of CA9 by shRNA demonstrated effective knockdown, particularly using shCA9#2 (Supplementary Figure 4*C*). Incubation of PK-8 cells with gemcitabine in normoxia significantly increased both glycolytic (Figure 4*C* and *D* and Supplementary Figure 4*D* and *E*) and mitochondrial function (Figure 4*E* and Supplementary Figure 4*F–I*), indicating the induction of a chemotherapy-induced stress response. CA9 depletion did not affect basal levels of glycolysis, but significantly inhibited the gemcitabine-induced increase in extracellular acidification rate (Figure 4*C* and *D* and Supplementary Figure 4*D* and *E*), whereas both basal and gemcitabine-induced mitochondrial function were impacted[23] (Figure 4*E* and Supplementary Figure 4*F–I*).

Next, we assessed similar parameters in PK-8 cells cultured in hypoxia, as HIF1A-mediated glucose metabolism has been previously implicated in resistance to gemcitabine.[24] Although levels of HIF1A increased with gemcitabine exposure, hypoxia-induced levels of CA9 expression were maximal and not further augmented (Figure 4*F*). Cells

Figure 3. CA9 depletion reduces tumor burden and dissemination in a *Kras*-driven mouse model of PDAC. (*A*) Immunohistochemistry for CA9 in KPCY GEMM tumors. Scale bar, 20 μm. (*B*) Immunohistochemical staining of serially sectioned tumor tissues from PENN 6620c1 orthotopic tumors. *Boxes*, regions shown at higher magnification. Scale bars, 100 μm (*top*); 20 μm (*bottom*). (*C*) Western blots of CA9 depletion by the PENN 6620c1 clone cultured for 72 hours in normoxia (N) or hypoxia (H). (*D*) Growth of CA9-depleted PENN 6620c1 cells cultured as spheroids. (n = 3, $^*P < .05$). (*E*) Images of mice with orthotopic pancreatic tumors derived from CA9-depleted 6620c1 cells 3 weeks postimplantation. (*F*) Quantification of total flux from animals in E (n = 5–6/group. $^{**}P < .01$). (*G*) pHi measurements for CA9-depleted 6620c1 cells cultured for 72 hours. (n = 6, $^*P < .05$, $^{***}P < .001$). (*H*) pHi measurements for 6620c1 cells incubated with SLC-0111 for 72 hours. (n = 3, $^*P < .05$, $^{**}P < .01$). (*I*) Invasion of CA9-depleted 6620c1 cells cultured for 72 hours. (n = 3, $^*P < .05$, ns = not significant).

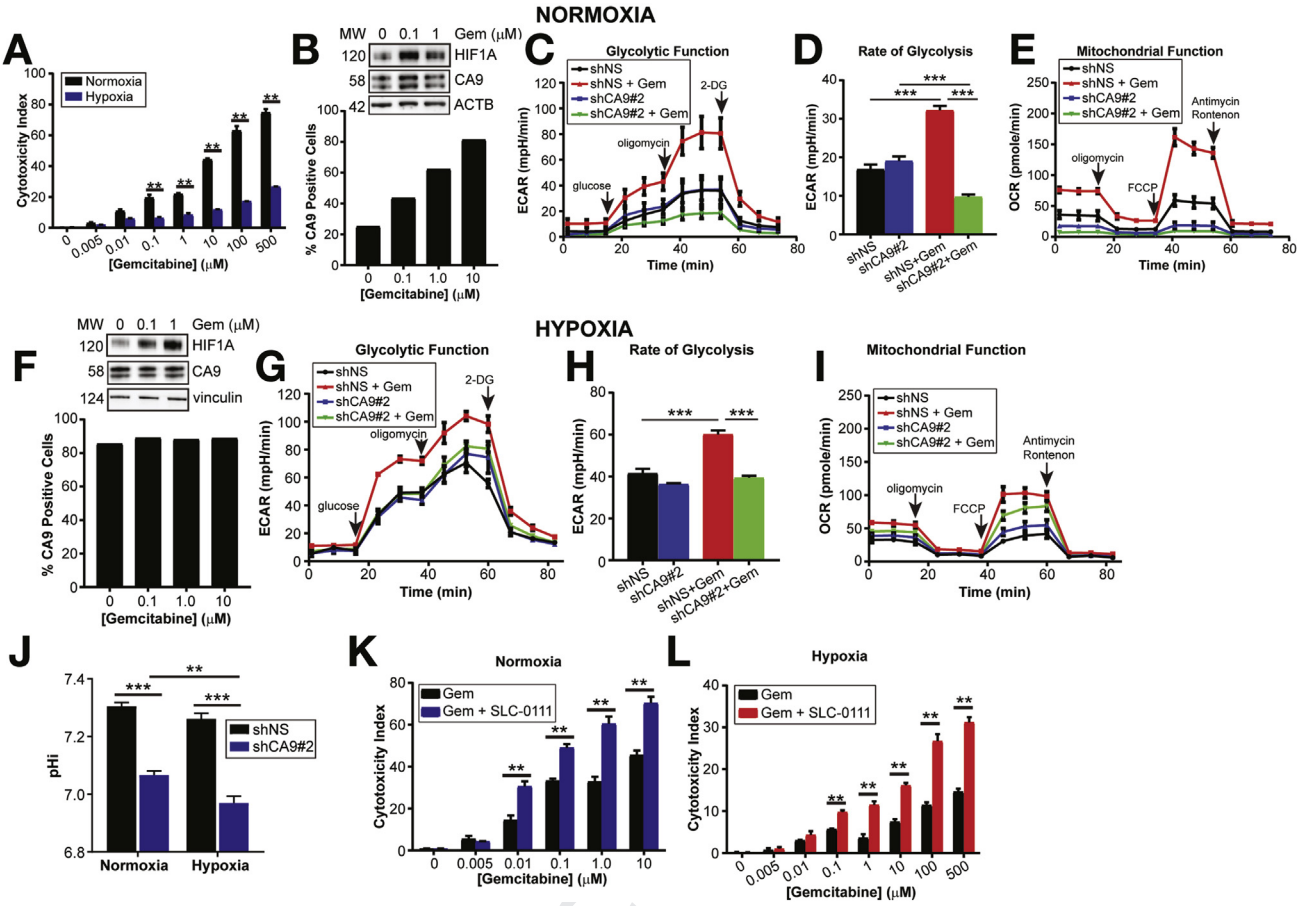

Figure 4. Inhibition of CA9 interferes with pH regulation and inhibits a gemcitabine-induced metabolic stress response. (*A*) Cytotoxicity of PK-8 cells incubated with gemcitabine for 72 hours (n = 3, $^{**}P < .01$). (*B–I*) PK-8 cells cultured for 48 hours in the indicated condition. (*B*) and (*F*), Western blots and FACS analysis of CA9 expression by cells incubated with gemcitabine for 48 hours in (*B*) normoxia or (*F*) hypoxia. (*C–E*) and (*G–I*) Metabolic flux analysis of CA9-depleted cells incubated with 20 μM gemcitabine for 48 hours in normoxia (*C–E*) and hypoxia (*G–I*). *Arrows*, compound addition. (*C*, *G*) Glycolytic stress test. (*D*, *H*) Rate of glycolysis (normoxia, n = 7, $^{***}P < .001$; hypoxia, n = 4, $^{**}P < .01$). (*E*, *I*) Mitochondrial stress test. (*J*) pHi measurements for CA9-depleted PK-8 cells cultured for 72 hours (n = 3, $^{*}P < .05$). (*K* and *L*) Cytotoxicity of PK-8 cells incubated for 72 hours with gemcitabine and 50 μM SLC-0111 in (*K*) normoxia (n = 3, $^{**}P < .01$) and (*L*) hypoxia (n = 3, $^{**}P < .01$).

demonstrated increased glycolysis (Figure 4*G* and *H* and Supplementary Figure 4*J* and *K*) and decreased mitochondrial function[23] (Figure 4*I* and Supplementary Figure 4*L–O*), compared with normoxia. Incubation with gemcitabine significantly increased glycolysis, an effect that was inhibited by depletion of CA9 (Figure 4*G* and *H*). Hypoxia also significantly exacerbated the acidification of pHi by CA9-depleted cells (Figure 4*J*). These data strongly suggest that inhibition of CA9 impairs the ability of these cells to regulate pHi and inhibits the chemotherapy-induced stress response, potentially increasing their vulnerability to gemcitabine.

Because gemcitabine exposure increases CA9 expression by PK-8 cells in normoxia (Figure 4*B*), we assessed whether pharmacologic inhibition of CA9 activity would enhance chemosensitivity. Cells were incubated with increasing concentrations of gemcitabine in the presence of 50 μM SLC-0111 and, congruent with the effect of CA9 depletion on gemcitabine-induced metabolic flux by these cells, incubation with the combination significantly increased cytotoxicity, compared to gemcitabine alone (Figure 4*K*; Supplementary Figure 5*A–C*).

We next incubated PK-8 cells in hypoxia. As expected given the relative resistance of these cells to gemcitabine in hypoxia (Figure 4*A*), the overall magnitude of the cytotoxic effect of gemcitabine and SLC-0111 in combination was reduced in hypoxia, compared with normoxia (Figure 4*K* and *L*); however, the combination was significantly more effective compared with gemcitabine alone (Figure 4*L* and Supplementary Figure 5*D*).

Finally, we determined whether incubation of PDAC cells with SLC-0111 also affected pHi homeostasis. PK-8 cells cultured in hypoxia for 72 hours to upregulate CA9, followed by incubation with 50 μM SLC-0111, resulted in a significant decrease in pHi (Supplementary Figure 5*E*). Importantly, incubation of CA9-negative Capan-2 human PDAC cells with SLC-0111 in hypoxia did not impact cell proliferation, whereas similar exposure of CA9-positive PK-8 cells significantly reduced growth, demonstrating inhibitor specificity (Supplementary Figure 5*F* and *G*). Thus, inhibition of CA9 impairs the metabolic response of PDAC cells to gemcitabine, indicating a potential mechanism for the observed enhancement of chemosensitivity by inhibition of CA9.

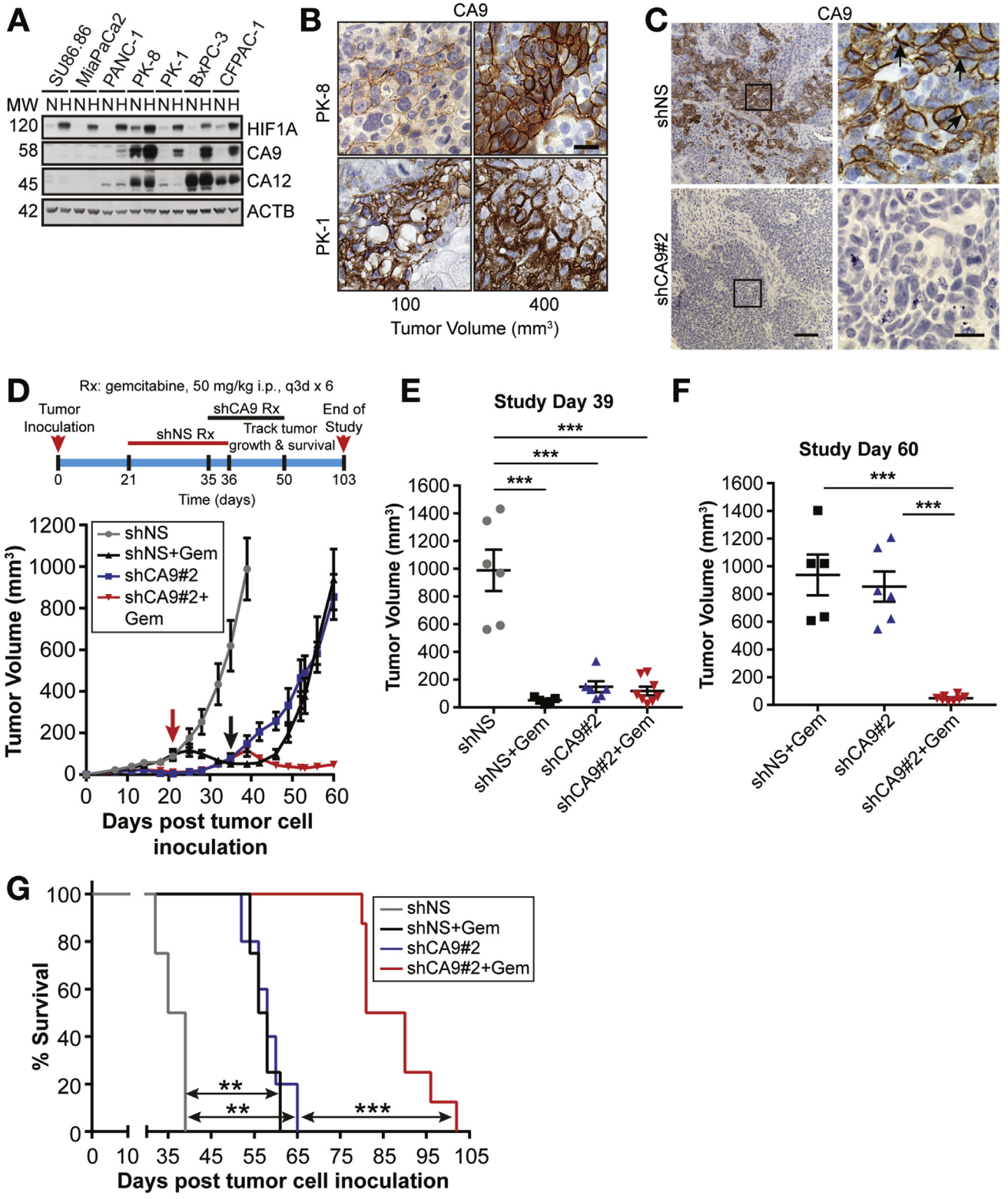

Figure 5. Combination of CA9 depletion and administration of gemcitabine enhances therapeutic efficacy in *KRAS*-driven PDAC xenografts. (*A*) Western blots of human PDAC cell lines cultured for 72 hours in normoxia (N) or hypoxia (H). (*B*) Immunohistochemistry for CA9 expression in PK-8 and PK-1 PDAC xenograft tumors. Scale bar = 20 μm. (*C*) Control and CA9-depleted PK-8 xenografts analyzed for CA9 by immunohistochemistry. *Boxes*, regions shown at higher magnification. Scale bars, 100 μm (*left*); 20 μm (*right*). (*D–G*) Control and CA9-depleted PK-8 xenografts administered gemcitabine. n = 4–8/group. (*D*) Study timeline and tumor growth curve. *Arrows*, start of drug administration. (*E*) Tumor growth when shNS tumors reached endpoint. ***$P < .001$. (*F*) Tumor growth when shNS + gemcitabine-exposed tumors reached endpoint. ***$P < .001$. (*G*) Kaplan-Meier curves (**$P < 0.01$, ***$P < .001$).

print & web 4C/FPO

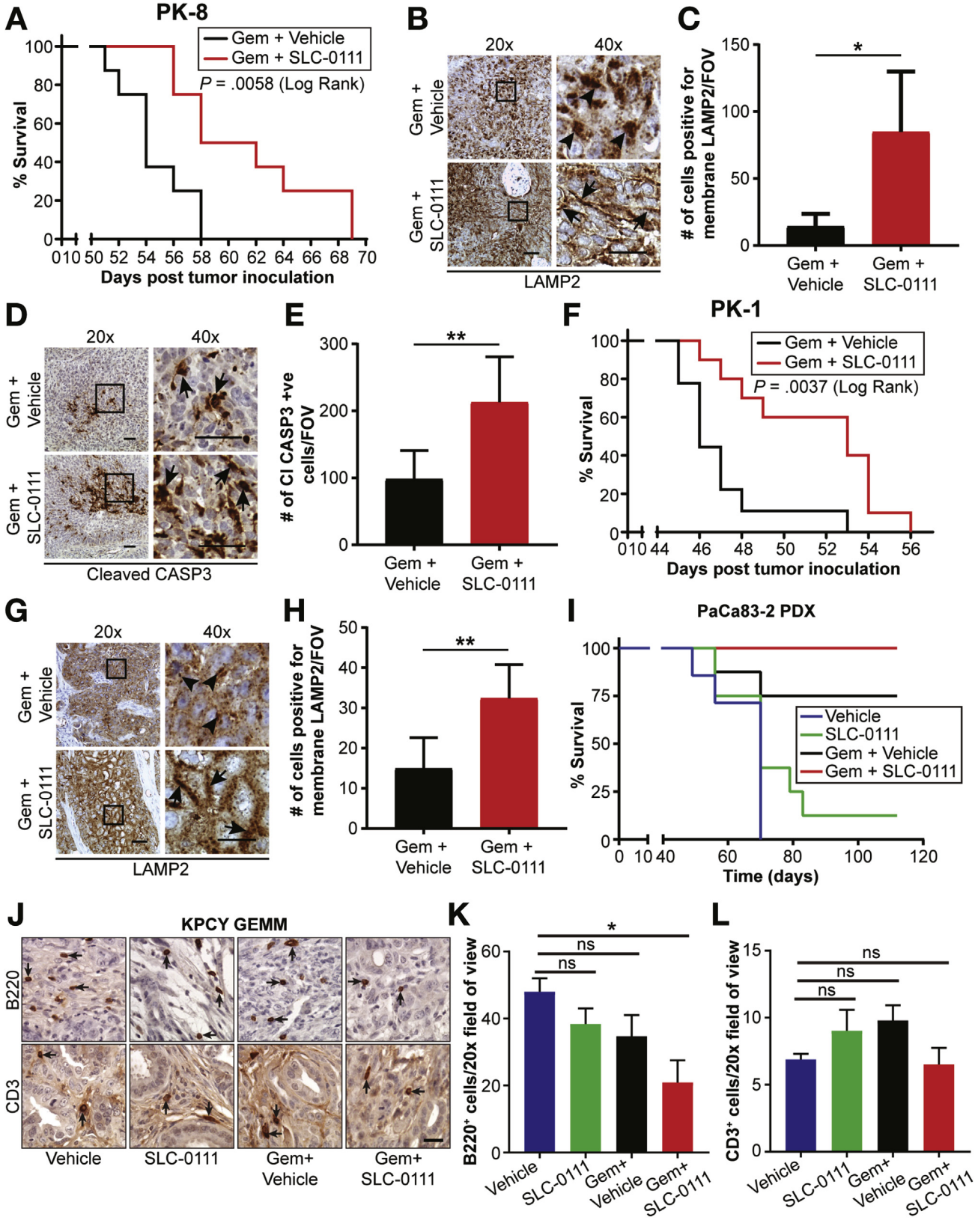

Combination of Genetic Depletion of CA9 Expression and Administration of Gemcitabine Enhances Therapeutic Efficacy in Models of KRAS-driven Human PDAC

Next, we wanted to determine whether silencing CA9 expression, in combination with gemcitabine administration, would elicit a superior therapeutic benefit in PDAC models in vivo. Levels of HIF1A and tumor-associated CAs were evaluated in a panel of human PDAC cell lines. All cell lines demonstrated increased levels of HIF1A expression in hypoxia and 4 of the 7 PDAC cell lines (58%) showed hypoxia-induced CA9 expression (Figure 5*A*), indicating that although PDAC cells generally upregulate CA9 in response to hypoxic stress, heterogeneity does exist and CA9 may be regulated independently of hypoxia-mediated HIF-1, for example by epigenetic mechanisms in a subset of PDAC cells.[14,25] CA12 was constitutively expressed to variable levels and was not induced by hypoxia (Figure 5*A*).

We selected cell lines that demonstrated robust hypoxia-induced upregulation of CA9, established tumors, and evaluated CA9 expression by immunohistochemistry. Tumors derived from *KRAS*-mutant PK-8 and PK-1 cell lines demonstrated tumor volume-dependent staining for CA9 expression (Figure 5*B*). We then established tumors from PK-8 cells depleted of CA9 expression and demonstrated that these tumors are negative for CA9 expression (Figure 5*C*).

Control and CA9-depleted PK-8 cells were implanted into mice, and animals with established tumors were administered gemcitabine (Figure 5*D*). When used individually, CA9 knockdown and gemcitabine administration significantly reduced tumor growth, compared with control tumors (Figure 5*D* and *E*). Furthermore, the combination of CA9 depletion and gemcitabine administration resulted in significant inhibition of tumor growth, compared with either intervention alone (Figure 5*D–F*).

CA9 depletion or injection of gemcitabine alone significantly increased survival, compared with vehicle control (Figure 5*G* and Supplementary Table 3). The combination regimen further enhanced efficacy by significantly extending survival compared with the single interventions (Figure 5*G* and Supplementary Table 3). All (100%) animals in the combination group were alive 65 days post inoculation, whereas no animals in each of the other groups were alive at this timepoint (Supplementary Table 3). These data provide proof of concept for a rational therapeutic strategy targeting CA9 together with gemcitabine.

Administration of SLC-0111 in Combination With Gemcitabine in KRAS-mutant PDAC In Vivo Prolongs Survival, Increases Intratumoral Acidosis and Enhances Tumor Cell Death

We evaluated the effects of SLC-0111 in combination with gemcitabine in CA9-positive, *KRAS*-mutant PDAC xenograft models. Administration of SLC-0111 and gemcitabine to PK-8 xenografts significantly reduced tumor growth, compared with gemcitabine alone (Supplementary Figure 6*A* and *B*). Furthermore, animals administered the combination demonstrated significantly increased survival (Figure 6*A*).

To determine whether inhibiting CA9 in combination with gemcitabine administration may lead to changes in intratumoral acidosis and cell viability, we evaluated the presence and distribution of lysosome-associated membrane protein 2 (LAMP2), a biomarker of tumor acidosis,[26] and cleaved caspase 3. LAMP2 was localized to perinuclear regions of the cytoplasm and showed a punctate expression pattern in tumors exposed to gemcitabine (Figure 6*B*), but shifted toward accumulation of membrane-localized expression (Figure 6*B*) with administration of the drug combination. The number of cells positive for membrane-localized LAMP2 expression increased significantly in these tumors (Figure 6*C*). We also observed a significant increase in cells positive for cleaved caspase 3 in tumors given the combination (Figure 6*D* and *E*).

Confirming our results, administration of both drugs to PK-1 PDAC xenografts significantly reduced tumor growth (Supplementary Figure 6*C* and *D*) and increased survival (Figure 6F), relative to gemcitabine alone. Although PK-1 cells upregulate CA9 (and CA12) to a lesser extent in vitro, when compared with PK-8 cells, PK-1 xenografts strongly express CA9 in vivo. Similarly, PK-1 xenografts exposed to gemcitabine showed a punctate pattern of LAMP2 staining (Figure 6*G*), whereas administration of the combination resulted in a significant increase in membrane-localized staining (Figure 6*G* and *H*).

To evaluate the efficacy of the drug combination on human tumors situated in a more clinically relevant microenvironment, we used an orthotopic PDX model of PDAC. Analysis of these tumors by immunohistochemistry revealed robust CA9 expression in several samples (Supplementary Figure 6*E*) and PaCa83–2 was selected for in vivo studies. Importantly, gemcitabine was administered to the patient as adjuvant chemotherapy and response to therapy was observed (Supplementary Table 4).

Figure 6. Administration of SLC-0111 in combination with gemcitabine in *KRAS*-mutant PDAC prolongs survival, increases intratumoral acidosis and enhances tumor cell death. (*A–E*) PK-8 and (*F–H*) PK-1 xenografts were injected with gemcitabine (50 mg/kg every 3 days, 6 doses), followed sequentially by daily administration of 50 mg/kg SLC-0111. (*A*) Kaplan-Meier curves (n = 8/group, $^{**}P = .0058$). (B) LAMP2 immunohistochemistry showing intracellular (*arrowheads*) and membrane (*arrows*) staining. Scale bars, 50 μm (*left*); 20 μm (*right*). (*C*) Quantification of LAMP2 expression (n = 4–5/group, $^{*}P < .05$). (*D*) Cleaved CASP3 immunohistochemistry (*arrows*). Scale bars, 50 μm (*left*); 20 μm (*right*). (*E*) Quantification of cleaved CASP3-positive cells (n = 6–7/group, $^{**}P < .01$). (*F*) Kaplan-Meier curves (n = 9–10/group, $^{**}P = .0037$). (*G*) LAMP2 immunohistochemistry as described in (*B*). Scale bars, 50 μm (*left*); 20 μm (*right*). (*H*) Quantification of LAMP2 expression (n = 6/group, $^{**}P < .01$). (*I*) Kaplan-Meier analysis of orthotopic PDX PaCa83 administered gemcitabine and SLC-0111. n = 6–8/group. (*J*) Images showing $B220^+$ and $CD3^+$ cells (*arrows*) in tumor sections from KPCY GEMM administered gemcitabine and SLC-0111. Scale bar, 20 μm. (*K* and *L*) Quantification of KPCY tumor sections for (*K*) $B220^+$ cells (n = 3–4/group, $^{*}P < .05$) and (*L*) $CD3^+$ cells (n = 3/group, $^{*}P < .05$, ns = not significant).

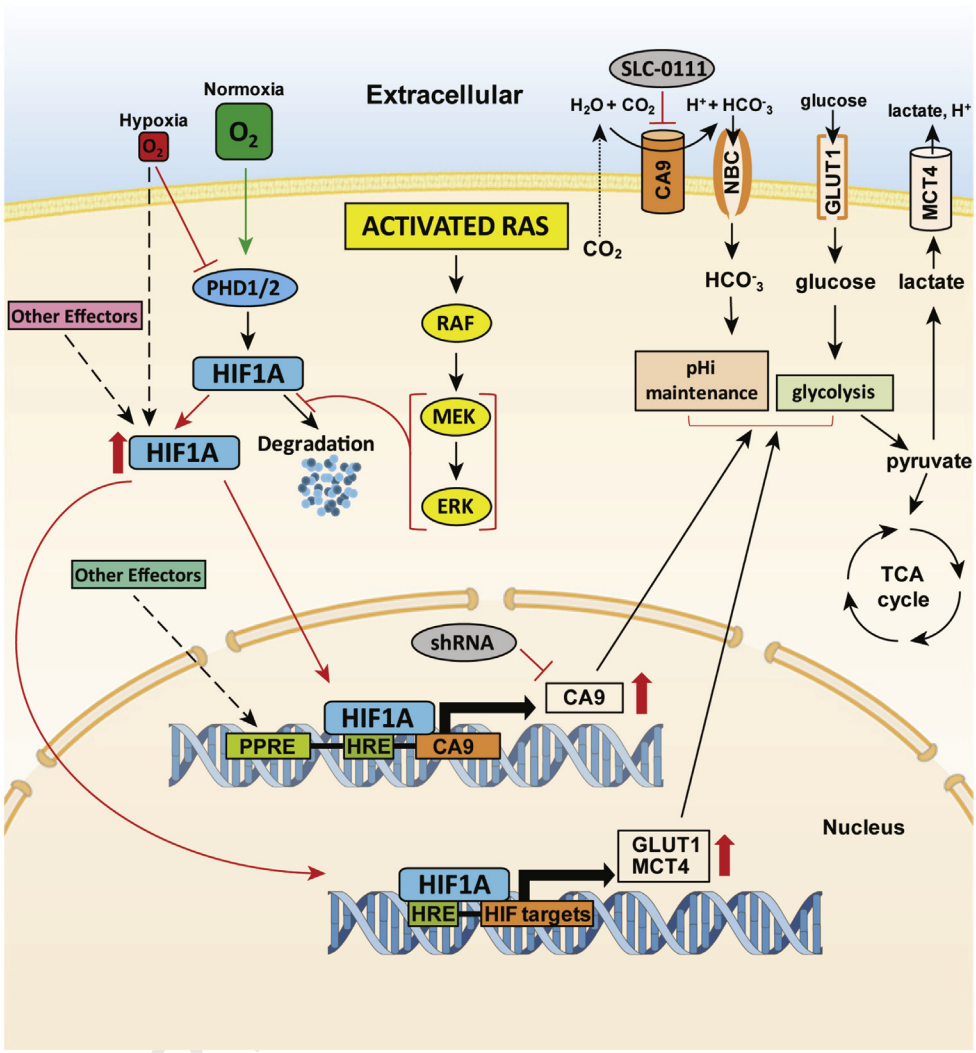

Figure 7. Schematic detailing pH regulation by CA9 as a therapeutically exploitable vulnerability of *KRAS*-driven PDAC. In addition to hypoxia, a major pathophysiologic stimulus for upregulation of CA9 in solid tumors, HIF1A expression can be stabilized/induced through other effectors and pathways, including PI3Kinase and mTOR, mutations in the TCA proteins such as fumerate hydratase, YB1, loss of VHL[32] and gemcitabine.

Control animals succumbed to disease within 70 days of initial drug administration, whereas some animals given SLC-0111 showed increased survival (Figure 6*I*). Analysis after 16 weeks demonstrated that although injection of gemcitabine alone extended survival compared with SLC-0111 or vehicle, administration of the drug combination resulted in a further increase in survival (Figure 6*I*) and 100% of given the combination were alive (Supplementary Table 5). One animal in this group remained tumor-free, whereas palpable tumors were observed in all animals in the other groups (Supplementary Table 5).

We used the KPCY GEMM to evaluate the potential impact of the drug combination on the immune microenvironment of PDAC tumors. Animals were given gemcitabine and SLC-0111 for 14 days, followed by immunohistochemical analysis for intratumoral B and T lymphocytes (Figure 6*J*–*L*). Administration of the combination resulted in a significantly fewer B220+ B cells, compared to control and single agents (Figure 6*K*), whereas there was no significant impact on the number of CD3+ T-cells (Figure 6*L*). These data show that the drug combination does not have an adverse impact on the immune micro environment and, in fact, may have a potentially beneficial effect by limiting the number of intrapancreatic B cells, a cell type that has recently been reported to promote pancreatic tumorigenesis.[27]

Discussion

The outcome of patients with pancreatic ductal adenocarcinoma remains dismal and there is a desperate need for the development of novel combinatorial therapeutic strategies that impinge specifically on the biology of PDAC tumors. Here, we have identified CA9 as a pharmacologically targetable vulnerability downstream of mutant KRAS, a highly penetrant mutation that occurs in the vast majority of PDACs. Importantly, this is the first in-depth report of a new therapeutic strategy targeting a hypoxia/pH-specific effector downstream of KRAS in combination with a standard of care chemotherapy in PDAC. Our data clearly show that the combination is superior to gemcitabine alone in several in vivo models of PDAC tumor growth and metastasis and suggest an innovative therapeutic approach in PDAC using a novel, nontoxic inhibitor of CA9 to sensitize cancer cells to chemotherapeutic agents.

We have used a spectrum of in vivo models of *KRAS*-driven PDAC, including a *Kras*-driven GEMM, multiple

human xenograft models as well as human PDX models to broadly evaluate the potential of targeting CA9. Our findings using genetic depletion strategies, as well as pharmacological inhibition of CA9 activity, demonstrate that CA9 inhibition leads to reduced tumor burden and metastatic dissemination, and dramatically extends survival. These data, especially the effect on survival of combining SLC-0111 with gemcitabine provide proof of concept for the potential of pharmacologic inhibition of CA9 to enhance the efficacy to gemcitabine-based chemotherapy in PDAC.

Our findings here show that KRAS, MEK, and ERK signaling exacerbate hypoxia-driven HIF1A and HIF2A protein stability, and that this leads to increased expression of downstream HIF1A-induced effectors such as CA9 and MCT4, concomitant with perturbation of pH regulation and metabolic rewiring toward a glycolytic phenotype (Figure 7).

A recent study reported that deleting HIF1A in a *Kras*-driven GEMM model resulted in accelerated neoplasia, attributed to an increase in the HIF1A-dependent B cell population.[27] Here we have found that although mutant KRAS regulates HIF1A stability in hypoxia, it is the contribution of the downstream effector, CA9, which promotes tumor growth and metastases because inhibiting CA9 has a major effect on KRAS-driven PDAC progression. Furthermore, administration of gemcitabine and SLC-0111 in combination to the KPCY GEMM model of PDAC resulted in fewer B cells in the tumor, suggesting that alterations to the immune environment of the tumor may be responsible for part of the observed efficacy. Because HIF1A regulates transcription of many genes, deleting HIF1A would be expected to lead to pleiotropic effects, including release of tumor suppressive pathways resulting in accelerated tumor growth, as demonstrated by Lee et al.[27] This suggests that targeting specific downstream effectors, such as CA9, rather that HIF1A per se, may be a more effective therapeutic strategy.

Our data suggest that HIF-1, downstream of KRAS, is a major driver of CA9 expression in the context of PDAC. Although we have not directly evaluated whether CA9 expression may be regulated by alternative pathways in response to acidosis, such as nuclear factor-κB activation,[28] we would expect that, because SLC-0111 has been shown to promote death of cancer cells in hypoxia/acidic conditions, PDAC cells upregulating CA9 by this mechanism would be targeted by the inhibitor.

Mechanistically, our in vitro and in vivo data demonstrate that hypoxia increases resistance of human PDAC cells to chemotherapeutic agents such as gemcitabine. This resistance can be overcome, in part, by adding the CA9 inhibitor to the therapeutic regimen, indicating that changes in pH regulation may underpin the increased efficacy observed with the drug combination. CA9 inhibition by PDAC cells in hypoxia decreases pHi, corroborated in vivo by tracking LAMP2 membrane translocation,[26] demonstrating that intracellular acidosis in response to CA9 inhibition is one potential mechanism by which sensitivity to gemcitabine is enhanced in these models.

Previous efforts to target CA9 clinically, for example in renal carcinoma, have used an antibody against CA9, girentuximab (cG250). A recent phase 3 trial using girentuximab as monotherapy in the adjuvant setting in patients with localized completely resected high-risk ccRCC failed to show clinical benefit compared with placebo.[29] Interestingly, subsequent analysis of a subset of patients with a high CA9 score revealed a trend toward an increase in disease-free survival, underscoring the importance of including CA9 expression within trial inclusion criteria.[29] In contrast, we observed efficacy of inhibition of CA9 activity when used in combination with chemotherapy in PDAC, and these data, together with observations showing efficacy of CA9 inhibition in combination with administration of temozolomide in preclinical models of glioblastoma[30] and melanoma models in vitro,[31] suggest that targeting CA9 in a combinatorial setting warrants further clinical investigation.

In conclusion, our findings identify a vulnerability of KRAS-driven pancreatic ductal adenocarcinomas resulting in a dependency on glycolysis and the need to buffer intracellular pH through the bicarbonate producing activity of CA9. Here we have identified and characterized a clinically tractable means of targeting CA9, resulting in increased intracellular acidosis and cell death with concomitant inhibition of tumor growth and dissemination.

Supplementary Material

Note: To access the supplementary material accompanying this article, visit the online version of *Gastroenterology* at www.gastrojournal.org, and at https://doi.org/10.1053/j.gastro.2019.05.004.

References

1. Siegel RL, Miller KD, Jemal A. Cancer statistics, 2019. CA Cancer J Clin 2019;69:7–34.
2. Kleeff J, Korc M, Apte M, et al. Pancreatic cancer. Nat Rev Dis Primers 2016;2:16022.
3. Cancer Genome Atlas Research Network. Integrated genomic characterization of pancreatic ductal adenocarcinoma. Cancer Cell 2017;32:185–203.e13.
4. Kimmelman AC. Metabolic dependencies in RAS-driven cancers. Clin Cancer Res 2015;21:1828–1834.
5. Infante JR, Somer BG, Park JO, et al. A randomised, double-blind, placebo-controlled trial of trametinib, an oral MEK inhibitor, in combination with gemcitabine for patients with untreated metastatic adenocarcinoma of the pancreas. Eur J Cancer 2014;50:2072–2081.
6. Nakazawa MS, Keith B, Simon MC. Oxygen availability and metabolic adaptations. Nat Rev Cancer 2016;16:663–673.
7. **Lohse I**, **Lourenco C**, Ibrahimov E, et al. Assessment of hypoxia in the stroma of patient-derived pancreatic tumor xenografts. Cancers (Basel) 2014;6:459–471.
8. Chiou SH, Risca VI, Wang GX, et al. BLIMP1 induces transient metastatic heterogeneity in pancreatic cancer. Cancer Discov 2017;7:1184–1199.
9. Xie H, Simon MC. Oxygen availability and metabolic reprogramming in cancer. J Biol Chem 2017;292:16825–16832.
10. Corbet C, Feron O. Tumour acidosis: from the passenger to the driver's seat. Nat Rev Cancer 2017;17:577–593.

11. Wilson WR, Hay MP. Targeting hypoxia in cancer therapy. Nat Rev Cancer 2011;11:393–410.
12. Chiche J, Ilc K, Laferriere J, et al. Hypoxia-inducible carbonic anhydrase IX and XII promote tumor cell growth by counteracting acidosis through the regulation of the intracellular pH. Cancer Res 2009; 69:358–368.
13. **Lou Y**, **McDonald PC**, Oloumi A, et al. Targeting tumor hypoxia: suppression of breast tumor growth and metastasis by novel carbonic anhydrase IX inhibitors. Cancer Res 2011;71:3364–3376.
14. Supuran CT, Alterio V, Di Fiore A, et al. Inhibition of carbonic anhydrase IX targets primary tumors, metastases, and cancer stem cells: Three for the price of one. Med Res Rev 2018;38:1799–1836.
15. **Li J**, **Byrne KT**, Yan F, et al. Tumor cell-intrinsic factors underlie heterogeneity of immune cell infiltration and response to immunotherapy. Immunity 2018; 49:178–193 e177.
16. Lock FE, McDonald PC, Lou Y, et al. Targeting carbonic anhydrase IX depletes breast cancer stem cells within the hypoxic niche. Oncogene 2013; 32:5210–5219.
17. El-Naggar AM, Veinotte CJ, Cheng H, et al. Translational activation of HIF1alpha by YB1 promotes sarcoma metastasis. Cancer Cell 2015;27:682–697.
18. **Qin R**, **Smyrk TC**, **Reed NR**, et al. Combining clinicopathological predictors and molecular biomarkers in the oncogenic K-RAS/Ki67/HIF-1alpha pathway to predict survival in resectable pancreatic cancer. Br J Cancer 2015;112:514–522.
19. Rhim AD, Mirek ET, Aiello NM, et al. EMT and dissemination precede pancreatic tumor formation. Cell 2012; 148:349–361.
20. McDonald PC, Swayampakula M, Dedhar S. Coordinated regulation of metabolic transporters and migration/invasion by carbonic anhydrase IX. Metabolites 2018; 8:E20.
21. **Swayampakula M**, **McDonald PC**, **Vallejo M**, et al. The interactome of metabolic enzyme carbonic anhydrase IX reveals novel roles in tumor cell migration and invadopodia/MMP14-mediated invasion. Oncogene 2017; 36:6244–6261.
22. Manji GA, Olive KP, Saenger YM, et al. Current and emerging therapies in metastatic pancreatic cancer. Clin Cancer Res 2017;23:1670–1678.
23. Khacho M, Tarabay M, Patten D, et al. Acidosis overrides oxygen deprivation to maintain mitochondrial function and cell survival. Nat Commun 2014;5:3550.
24. **Shukla SK**, **Purohit V**, **Mehla K**, et al. MUC1 and HIF-1alpha signaling crosstalk induces anabolic glucose metabolism to impart gemcitabine resistance to pancreatic cancer. Cancer Cell 2017;32:392.
25. Jakubickova L, Biesova Z, Pastorekova S, et al. Methylation of the CA9 promoter can modulate expression of the tumor-associated carbonic anhydrase IX in dense carcinoma cell lines. Int J Oncol 2005; 26:1121–1127.
26. Damaghi M, Tafreshi NK, Lloyd MC, et al. Chronic acidosis in the tumour microenvironment selects for overexpression of LAMP2 in the plasma membrane. Nat Commun 2015;6:8752.
27. Lee KE, Spata M, Bayne LJ, et al. Hif1a Deletion Reveals Pro-Neoplastic Function of B Cells in Pancreatic Neoplasia. Cancer Discov 2016;6:256–269.
28. Andreucci E, Peppicelli S, Carta F, et al. Carbonic anhydrase IX inhibition affects viability of cancer cells adapted to extracellular acidosis. J Mol Med (Berl) 2017; 95:1341–1353.
29. Chamie K, Donin NM, Klopfer P, et al. Adjuvant Weekly Girentuximab Following Nephrectomy for High-Risk Renal Cell Carcinoma: The ARISER Randomized Clinical Trial. JAMA Oncol 2017;3:913–920.
30. **Boyd NH**, **Walker K**, Fried J, et al. Addition of carbonic anhydrase 9 inhibitor SLC-0111 to temozolomide treatment delays glioblastoma growth in vivo. JCI Insight 2017;2:92928.
31. Andreucci E, Ruzzolini J, Peppicelli S, et al. The carbonic anhydrase IX inhibitor SLC-0111 sensitises cancer cells to conventional chemotherapy. J Enzyme Inhib Med Chem 2019;34:117–123.
32. Kroemer G, Pouyssegur J. Tumor cell metabolism: cancer's Achilles' heel. Cancer Cell 2008;13:472–482.

Author names in bold designate shared co-first authorship.

Received November 7, 2018. Accepted May 6, 2019.

Reprint requests
Address requests for reprints to: Shoukat Dedhar, PhD, Department of Integrative Oncology, BC Cancer Research Centre, 675 West 10th Avenue, Vancouver, BC, V5Z 1L3, Canada. e-mail: sdedhar@bccrc.ca; fax: 604–675–8099.

Acknowledgments
We thank Andrew Metcalfe and Dr Cynthia Clendenin for expert technical assistance with the PDX surgeries and the KPCY GEMM studies, respectively. We gratefully acknowledge the participation of the patients and the Personalized Oncogenomics team. Published results here are in part based on data generated by the Personalized Oncogenomics Program: http://www.personalizedoncogenomics.org/.

Author Contributions:Conception and design: P.C. McDonald, S.C. Chafe, W.S. Brown, D.J. Renouf, S. Dedhar; Development of methodology: P.C. McDonald, S.C. Chafe, W.S. Brown, M. Swayampakula, D.T. Yapp, J. Li; Acquisition of data (provided animals, acquired and managed patient data, provided facilities, etc.): P.C. McDonald, S.C. Chafe, W.S. Brown, S. Saberi, M. Swayampakula, G. Venkateswaran, O. Nemirovsky, J.A. Gillespie, J.M. Karasinska, S.E. Kalloger, C.T. Supuran, D.F. Schaeffer, A. Bashashati, S.P. Shah, J.T. Topham, D.T. Yapp, J Li, D.J. Renouf, B.Z. Stanger, S. Dedhar; Analysis and interpretation of data (eg, statistical analysis, biostatistics, computational analysis): P.C. McDonald, S.C. Chafe, W.S. Brown, M. Swayampakula, G. Venkateswaran, O. Nemirovsky, S.E. Kalloger, D.F. Schaeffer, S. Saberi, A. Bashashati, B.Z. Stanger, S. Dedhar; Writing, review and/or revision of the manuscript: P.C. McDonald, S.C. Chafe, W.S. Brown, B.Z. Stanger, S. Dedhar; Administrative, technical, or material support (ie, reporting or organizing data, constructing databases): J.M. Karasinska; Study supervision: P.C. McDonald, S.C. Chafe, W.S. Brown, S. Dedhar.

Conflicts of interest
These authors disclose the following: P.C.M., C.T.S., and S.D. are inventors of SLC-0111. The remaining authors disclose no conflicts.

Funding
This work was supported by grants to SD from the Canadian Cancer Society Research Institute (CCSRI grant 703191), the Canadian Institutes of Health Research (CIHR grant FDN-143318), and funding from Pancreas Centre BC, BC Cancer Foundation, and VGH Foundation.